Оригинальные статьи

Original papers

УДК 544.7+576

LUMINESCENT QUANTUM DOTS ENCAPSULATED BY ZWITTERIONIC AMPHIPHILIC POLYMER: SURFACE CHARGE-DEPENDENT INTERACTION WITH CANCER CELLS

***E. A. PETROVA*[a], *T. I. TERPINSKAYA*[a], *A. A. FEDOSYUK*[b], *A. V. RADCHANKA*[b], *A. V. ANTANOVICH*[b], *A. V. PRUDNIKAU*[b], *M. V. ARTEMYEV*[b]**

[a]*Institute of Physiology, National Academy of Sciences of Belarus, 28 Akademičnaja Street, Minsk 220072, Belarus*
[b]*Research Institute for Physical Chemical Problems, Belarusian State University, 14 Lieninhradskaja Street, Minsk 220006, Belarus*

Corresponding author: M. V. Artemyev (m_artemyev@yahoo.com)

Here, we prepared water-soluble highly luminescent CdSe/ZnS quantum dots having different surface charge and examined how zeta potential of quantum dots affected their uptake by cancer cells. Water soluble quantum dots with varied zeta potential were prepared through encapsulation with amphiphilic polymer poly(maleic anhydride-alt-1-tetradecene) (PMAT) containing ziwitterions formed by spatially separated carboxyl and quaternary amino groups. Varying the ration

Образец цитирования:
Петрова Е. А., Терпинская Т. И., Федосюк А. А., Радченко А. В., Антанович А. В., Прудников А. В., Артемьев М. В. Люминесцентные квантовые точки, инкапсулированные цвиттер-ионным амфифильным полимером: влияние поверхностного заряда на взаимодействие с опухолевыми клетками // Журн. Белорус. гос. ун-та. Химия. 2018. № 1. С. 3–13 (на англ.).

For citation:
Petrova E. A., Terpinskaya T. I., Fedosyuk A. A., Radchanka A. V., Antanovich A. V., Prudnikau A. V., Artemyev M. V. Luminescent quantum dots encapsulated by zwitterionic amphiphilic polymer: surface charge-dependent interaction with cancer cells. *J. Belarus. State Univ. Chem.* 2018. No. 1. P. 3–13.

Авторы:
Елена Александровна Петрова – научный сотрудник.
Татьяна Ильинична Терпинская – научный сотрудник.
Александра Александровна Федосюк – младший научный сотрудник.
Александра Валерьевна Радченко – студентка химического факультета. Научный руководитель – М. В. Артемьев.
Артем Владимирович Антанович – младший научный сотрудник.
Анатолий Викторович Прудников – младший научный сотрудник.
Михаил Валентинович Артемьев – заведующий лабораторией.

Authors:
Elena A. Petrova, researcher.
helena_iseu@mail.ru
Tatiana I. Terpinskaya, researcher.
terpinskayat@mail.ru
Aleksandra A. Fedosyuk, junior researcher.
sasha-f18@mail.ru
Aliaksandra V. Radchanka, student at the faculty of chemistry.
sasha-f18@mail.ru
Artsiom V. Antanovich, junior researcher.
antanovi4@gmail.com
Anatol V. Prudnikau, junior researcher.
nanochem@mail.ru
Mikhail V. Artemyev, head of the laboratory.
m_artemyev@yahoo.com

of negatively charged carboxyl and positively charged quaternary amino-groups during chemical modification of PMAT we control the sign and magnitude of zeta potential of encapsulated quantum dots. Quantum dots having nearly equal amount of carboxyl and quaternary amino groups possess pH-controlled zeta potential which can vary from negative to positive value when pH changes from basic to acidic condition. Cellular uptake of encapsulated quantum dots has been found to be strongly dependent of their surface charge: positively charged quantum dots efficiently internalized by cells, while negatively charged adsorbed mostly at the cell membrane. Zwitterionic QDs do not demonstrate any charge-dependent cellular toxicity at least within few hours. Long-term incubation of cells stained with zwitterionic quantum dots results in the decrease of the fluorescence signal mainly due to the cell proliferation.

Key words: quantum dots; zwitterion; zeta potential; nanoparticle uptake.

Acknowledgements. Authors acknowledge partial financial support from CHEMREAGENTS and Convergence programs.

ЛЮМИНЕСЦЕНТНЫЕ КВАНТОВЫЕ ТОЧКИ, ИНКАПСУЛИРОВАННЫЕ ЦВИТТЕР-ИОННЫМ АМФИФИЛЬНЫМ ПОЛИМЕРОМ: ВЛИЯНИЕ ПОВЕРХНОСТНОГО ЗАРЯДА НА ВЗАИМОДЕЙСТВИЕ С ОПУХОЛЕВЫМИ КЛЕТКАМИ

Е. А. ПЕТРОВА [1)], ***Т. И. ТЕРПИНСКАЯ*** [1)], ***А. А. ФЕДОСЮК*** [2)], ***А. В. РАДЧЕНКО*** [2)], ***А. В. АНТАНОВИЧ*** [2)], ***А. В. ПРУДНИКОВ*** [2)], ***М. В. АРТЕМЬЕВ*** [2)]

[1)] *Институт физиологии НАН Беларуси, ул. Академическая, 28, 220072, г. Минск, Беларусь*
[2)] *Учреждение БГУ «Научно-исследовательский институт физико-химических проблем», ул. Ленинградская, 14, 220006, г. Минск, Беларусь*

На основе приготовленных водных коллоидных растворов люминесцентных квантовых точек CdSe/ZnS, имеющих различный поверхностный заряд, исследовано, как дзета-потенциал квантовых точек влияет на их поглощение опухолевыми клетками. Водорастворимые квантовые точки с варьируемым дзета-потенциалом получены посредством инкапсуляции амфифильным полимером – полималеиновым ангидрид-альт-1-тетрадеценом (ПМАТ), содержащим цвиттер-ионы, образованные пространственно разделенными карбоксильными и четвертичными аммонийными группами. Варьируя соотношение отрицательно заряженных карбоксильных и положительно заряженных четвертичных аммонийных групп в процессе химической модификации ПМАТ, можно контролировать знак и величину дзета-потенциала инкапсулированных квантовых точек. Квантовые точки, несущие на поверхности примерно равное количество карбоксильных и четвертичных аммонийных групп, обладают pH-зависимым дзета-потенциалом, который может изменяться от отрицательного до положительного значения при переходе от щелочной среды к кислой. Обнаружено, что поглощение клетками инкапсулированных квантовых точек существенно зависит от их поверхностного заряда: положительно заряженные поглощаются клетками, тогда как отрицательно заряженные главным образом адсорбируются на их мембране. Цвиттер-ионные квантовые точки не проявляют заметной цитотоксичности по крайней мере в течение нескольких часов. Длительная инкубация клеток, меченных цвиттер-ионными квантовыми точками, приводит к уменьшению люминесцентного сигнала, что в значительной мере обусловлено клеточной пролиферацией.

Ключевые слова: квантовые точки; цвиттер-ион; дзета-потенциал; поглощение наночастиц.

Благодарность. Авторы выражают благодарность за частичную финансовую поддержку государственных программ научных исследований «Химреагенты» и «Конвергенция».

Introduction

Semiconductor colloidal nanocrystals or quantum dots (QDs) with size-tunable optical properties have found numerous applications in biological assays and detection platforms [1–4]. Such QDs are primarily prepared in organic solvents at high temperatures and, hence, are covered with hydrophobic ligands. In order to use such particles in biological systems, QDs are required to be soluble in water, what can be achieved by additional post-synthetic treatment. In order to promote transfer of QDs into aqueous buffer solutions several strategies were developed, the majority of which can be essentially divided into two main categories: polymer encapsulation and ligand exchange [5–7]. Utilization of amphiphilic polymers as solubilizing agents

provides colloidal stability of nanoparticles (NPs) in aqueous solutions, allows controlling hydrodynamic size and surface charge of NPs and also enables introduction of functional groups that can be further utilized for chemical functionalization of NPs' surface [5; 6; 8–10].

Surface charge of NPs is a key parameter that determines their colloidal stability, interaction with macromolecules and cell surfaces and influences NPs' performance in a variety of biomedical assays [11–14]. Utilization of amphiphilic polymers based on poly(maleic anhydride) for encapsulation of NPs has demonstrated promising opportunities for engineering of NCs' coating that can be implemented in biolabeling. While NCs' shape and size significantly contribute to their interaction with cells, the nature of functional groups on the NPs' surface plays the major role [12; 14]. While NCs encapsulated with non-modified poly(maleic anhydride) derivatives possess negative charge provided by carboxyl groups on their surface, it is possible to prepare through certain polymer modification NPs with desirable surface functional groups and charge.

Earlier, poly(ethylene glycol) (PEG)-decorated poly(maleic anhydride) derivatives have been reported to reduce non-specific and prevent protein adsorption [6]. Due to its relative inertness and hydrophilic nature, PEG is widely used to provide biocompatibility to polymers and various NPs [15–18]. Overall neutral surface charge on nanoparticles can also be obtained through the surface modification of nanoparticles with zwitterionic ligands by ligand exchange technique [7; 18–21] or encapsulation methods [22; 23]. Strong interaction of the zwitterions with water molecules can also provide good NPs biocompability. In comparison to PEG, zwitterions provide smaller hydrodynamic size of NPs and contain both positively and negatively charged groups that provide an overall neutral charge. This, in turn, prevents particles from aggregation via interaction with various charged species that are always present in biological media.

Recently QDs encapsulated with poly(maleic anhydride-alt-1-tetradecene) (PMAT) partially functionalized with N,N-dimethylethylenediamine were used as intracellular labels with proton-sponge properties [22]. Polymer modification with ternary amino compound allowed preparation of QDs with surface charge that depends on the number of introduced ternary amino and remaining carboxyl groups in the polymer coating. On the other hand, diamine functionalization of PMAT-encapsulated QDs that carry surface carboxyl groups often results in their aggregation in aqueous solution due to electrostatic charge screening and charge neutralization. In current work we utilize another strategy that consists in controlled modification of PMAT in organic solution using quaternary amino-compound ((2-aminoethyl)trimethylammonium chloride) and subsequent encapsulation of highly luminescent CdSe/ZnS core-shell QDs with obtained zwitterionic polymer. Since quaternary amino group provides pH-independent positive surface charge, total zeta potential of encapsulated QDs may be a simple function of pH and the ratio of the number of carboxyl groups to the number of quaternary amino groups on the surface of QDs. Remaining carboxyl groups of PMAT provide pH-dependent local negative charge on the surface of QDs. We prepared two types of quaternary amine-modified PMAT that have positive (+) and close to neutral (+/−) zeta potential and examined the effect of QDs' charge on cellular interactions and nonspecific binding with living cells (Ehrlich Ascites Carcinoma (EAC), human leucocytes, rat glioma C6). Investigation of the correlation between the physical and chemical properties of QDs and their cellular uptake is essential for understanding and controlling these interactions [24–28]. The information on QDs excretion is also very essential, since it determines the intensity of the fluorescent signal in labeled cells and allows tracking their pathways within cell using optical microscopy [29].

Materials and methods

Materials. *Chemicals.* Poly(maleic anhydride-alt-1-tetradecene) (PMAT, MW = 9000), (2-aminoethyl)trimethylammonium chloride hydrochloride (AETA), N-(3-dimethylaminopropyl)-N′-ethylcarbodiimide (EDC), NaOH, 1-hexanethiol, anhydrous chloroform, cellulose acetate membrane (cut-off = 12 kDa) were purchased from Sigma-Aldrich. 7-Aminoactinomycin (7-AAD), propidium iodide (PI), Hoechst 33342, Trypan blue were purchased from Sigma. Cell TraceViolet (CTV) was purchased from Molecular Probes.

Cell culture media and supplements. Hanks' balanced salt solution (HBSS), phosphate buffered saline (PBS), high glucose Dulbecco's modified Eagle's medium (DMEM), trypsin-EDTA solution, antibiotic-antimycotic solution (100×) with 10,000 units penicillin, 10 mg streptomycin and 25 μg amphotericin B per ml were purchased from Sigma-Aldrich. Sodium pyruvate (100×) was purchased from Gibco by Life Technologies, USA. Fetal calf serum (FCS) was purchased from HyClone, Thermo Scientific, UK.

Modification of PMAT with quaternary amine AETA (PMAT-AETA). For the preparation of (+/−) or (+) QDs 18 or 53 mg of AETA respectively was dissolved in 5 mL of dry dioxane at 80 °C. After 20 min 30 mg PMAT was added to the dioxane solution and the mixture was stirred at 80 °C for 3 h. Then EDC was added in a 4-fold excess to AETA and the reaction mixture was then stirred at 50 °C for additional 2 h. After that the solution was cooled down to room temperature and stirred overnight in order to complete the

reaction of PMAT carboxyl groups with AETA. After that dioxane was evaporated at 50 °C and the solid phase was dissolved in aqueous solution of NaOH with pH 12. Modified polymer was purified from the excess of small molecules by overnight dialysis against distilled water at room temperature using cellulose acetate membrane.

After the purification modified polymer was dried at 60 °C and redissolved in anhydrous chloroform. Concentration of the modified PMAT in chloroform was determined on the basis of the initial amount of the polymer introduced into reaction. Resultant solution was filtered through 0.2 μm Nylon membrane and stored at +4 °C in dark.

Synthesis, encapsulation and characterization of QDs. CdSe/ZnS core-shell QDs with core diameter of 2.9 nm and emission peak at λ = 570 nm were synthesized according to standard procedure. NCs were purified by precipitation with isopropanol and redissolved in chloroform. Average surface area of QDs was calculated from the average diameter of corresponding core-shell NCs that was determined using transmission electron microscopy (TEM). TEM samples were prepared by drying a droplet of the chloroform solution of NCs on carbon-coated copper grids. TEM micrographs were acquired using LEO 906E transmission electron microscope.

In order to achieve stable and reproducible results during encapsulation, the surface of QDs was capped with hexanethiol via ligand-exchange procedure. To ensure complete encapsulation of QDs with polymer, the total amount of the added polymer was in a 2.5-fold weight excess to QDs. For encapsulation the mixture of polymer and QDs was stirred for 24 h and dried at room temperature. Resultant glass-like solid phase of encapsulated QDs along with the excess of polymer was dissolved in distilled water or aqueous NaOH solution with pH 12 and centrifuged at 10 000 rpm for 5 min to remove insoluble residuals. The excess of polymer was removed from aqueous colloidal solutions of encapsulated QDs by ultrafiltration through commercial fiber membrane filter with cut-off ≈ 100 kDa and subsequent dialysis against distilled water. Finally, the solution was filtered through 0.2 μm Nylon membrane.

Concentration of CdSe/ZnS QDs encapsulated with PMAT was determined using molar extinction coefficient of corresponding core NCs from the reference data. Zeta potential of encapsulated colloidal NCs in different buffers was measured using Malvern Zetasizer Nano ZS90 instrument.

Cells. *Ehrlich Ascites Carcinoma*. EAC cells were maintained by weekly serial intraperitoneal transplantation, freshly drawn from a donor. The EAC cells were isolated from the peritoneal cavity of mice bearing 8-day-old ascites tumors. The cells were washed twice and resuspended in HBSS. The viability of EAC cells was more than 95 % as determined by propidium iodide/7-AAD exclusion (flow cytometry). We followed World Health Organization's International Guiding Principles for Biomedical Research involving Animals.

Human leucocytes. Leucocytes were separated from heparinized venous blood by lyzing erythrocytes in a solution containing 155 mmol/L ammonium chloride, 10 mmol/L sodium bicarbonate and 0.1 mmol/L EDTA for 10 min. The leucocyte fraction was washed twice and resuspended in HBSS. Isolated leucocytes were used in the experiments immediately. Leucocytes viability was more than 90 % as determined by propidium iodide or 7-AAD exclusion (flow cytometry).

QDs-cell interaction. *QDs uptake and short-time toxicity.* EAC cells or leucocytes suspensions (in HBSS, unless stated otherwise) were transferred into 96-well round-bottom plate. After that, QDs were introduced in the amount necessary to achieve the final concentration of 0.1–0.3 μmol/L of nanoparticles and then plates were incubated for 0.5 h. Cellular uptake of QD was measured using flow cytometry (PE-A channel) and QD distribution in cells was visualized with fluorescent microscope. Cell viability was determined by 7-AAD exclusion (flow cytometry).

QDs long-term toxicity and elimination. We analyzed the changes in the fluorescent signal from cells stained with QD or dye CTV. EAC cells were stained in HBSS with CTV according to the manufacturer's manual or with QDs for 20 min, washed twice in HBSS and resuspended in DMEM containing 10 % FBS and antibiotic-antimycotic. Cells were cultivated on 24-well plate (Greiner, Austria) for 2 days at 37 °C in CO_2 incubator (Shellab, USA) with CO_2 level of 5 %. After 0.5, 4, 24, 28, 48 h of incubation the aliquots of the cell suspension were drawn and used for flow cytometry analysis. Cells viability was investigated using 7-AAD test. QDs and CTV fluorescence intensity was registered only for living cells.

Instrumental analysis. *Flow cytometry.* Flow cytometry analysis was performed using BD FACSCanto II and Diva 7.0 software (Becton Dickinson, USA). Gating of human leucocytes based on FSC/SSC was performed to separate granulocytes, monocytes and lymphocytes.

Optical microscopy. A suspension of EAC cells was placed on a glass plate and optical images were obtained using Leitz MPV-2 and Opton microscopes with 16× and 25× objectives. Mercury lamp was used for fluorescence excitation (λ = 365 nm) and PLOEMOPAK system with emission filters at 370–490 and

520–700 nm range were used for the registration of fluorescence images. The images were registered with Leica DC300 F digital camera controlled by Leica IM1000 software.

For nuclei visualization cells were stained with 10^{-5} mol/L Hoechst 33342 in PBS (20 °C, 15–30 min).

Fluorescence quenching by Trypan blue. Fluorescence intensity of stained cells was registered at first in the absence of Trypan blue and then 5 min after the addition of 1 % solution of Trypan blue. Trypan blue fluorescence was registered at PerCP-Cy5.5-A channel, while QDs fluorescence registered at PE-A channel. Dead cells which have been Trypan blue-positive were excluded from analysis. Trypan blue-induced fluorescence quenching of membrane-associated QDs was measured in living cells only.

Statistical analysis. Statistical analysis was performed using Excel Software and Statistics 7. The deviations were considered significant for p values < 0.05 according to the Mann – Whitney test. Experimental points are presented as the mean values ± SEM.

Results and discussion

Figure 1 schematically demonstrates the formation zwitterions via PMAT modification with AETA and the structure of encapsulated QDs.

Figure 1 shows that during encapsulation chemically modified PMAT creates hydrophobic bilayer on the surface of CdSe/ZnS Ds via Van der Waals interaction of C12 aliphatic side chains of PMAT and hexanetiol bound to the surface Zn atoms of QDs. Pairs of carboxyl and quaternary amino groups on the surface of PMAT nano-capsule create spatially separated zwitterions with the negative charge of carboxyl groups partially or fully compensated by positive charge of amino groups. Overall zeta potential of encapsulated QDs depends on the ratio of carboxyl and quaternary amino groups. Table 1 represents characteristics of QDs encapsulated with three different PMAT-based polymers.

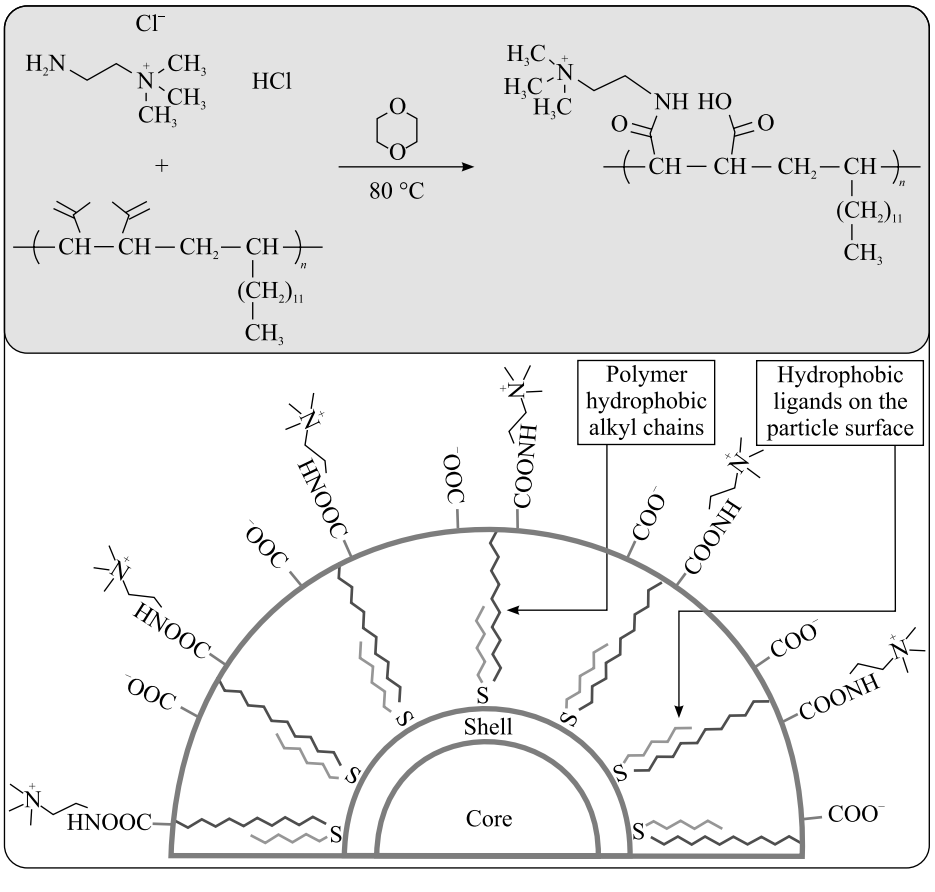

Fig. 1. Scheme of the formation of zwitterions by the chemical modification of PMAT with quaternary amine AETA (top) and the structure of highly luminescent CdSe/ZnS QDs encapsulated with zwitterion-containing PMAT (bottom). The ratio of carboxyl and quaternary amino groups can be tuned from 0 % for (−)QDs to 50 % for (+/−)QDs and to nearly 100 % for (+)QDs

Table 1

Zeta potential and hydrodynamic size determined by DLS-measurements of CdSe/ZnS QDs encapsulated with three different types of polymers: pure PMAT (−), PMAT fully (+) and partially (+/−) functionalized with quaternary amine AETA (MES buffer, pH 7.4)

QDs sample name	ζ-Potential, mV	Hydrodynamic size, nm
(−)QDs	−40	14
(+)QDs	+30	22
(+/−)QDs	−4	18

The data in table 1 shows that QDs encapsulated with pure PMAT ((−)QDs) show strongly negative surface charge due to the dissociation of surface carboxyl groups. QDs encapsulated with 100 % AETA-modified PMAT ((+)QDs) show large positive surface charge, while 50 % modified PMAT ((+/−)QDs) possess nearly zero zeta potential at pH 7.4. Hydrodynamic size of all encapsulated QDs was around 15–20 nm.

To determine optimal conditions for further comparative experiments, we initially measured the uptake of QDs by tumor cells in different buffers. The uptake of (−)QDs by tumor cells is sensitive to the presence of Ca^{2+} and less sensitive to Mg^{2+} in the solution. Ca/Mg-free PBS buffer affords weak staining, as well as PBS with glucose. However, the addition of Mg^{2+} increases (−)QDs binding threefold and Ca^{2+} – almost fivefold. Since Hank's buffer is based on PBS with added Ca^{2+}, Mg^{2+} and glucose, HBSS is more suitable for staining live cells with (−)QDs than standard PBS. Addition of fetal bovine serum remarkably inhibits (−)QDs uptake by tumor cells.

Earlier, T. Geelen et al. [30] on the example of mouse macrophages (RAW cells) demonstrated that Ca- and Mg-ions in incubation media provide efficient uptake of phosphatidylserine-containing paramagnetic liposomes. Authors suggested the major role in the uptake of Ca^{2+}-dependent receptors involved in the recognition of apoptotic cells expressing phosphatidylserine, such as, LOX-1 (lectin-like oxidized low-density lipoprotein receptor-1) scavenger receptor, whose calcium-dependent nature was revealed by J. E. Murphy et al. [31]. In our work we used different cell type and QDs used in this study were not conjugated to phosphatidylserine and thus another explanation of the increased QDs uptake in the presence of Ca^{2+} and Mg^{2+} ions was proposed. Investigation of neurotransmission demonstrated that Ca^{2+} ions are involved in the regulation of vesicular transport of neurotransmitters [32]. All this data suggests that Ca^{2+} ions are possibly involved in the regulation of vesicular transport of nanoparticles. However, detailed analysis of the ion-dependent transport is beyond the scope of current paper.

After that we compared the efficiency of cellular uptake of encapsulated QDs with different surface charge. Figure 2 shows fluorescence images of EAC cells stained with differently charged (−)QDs and (+)QDs.

The influence of zeta potential on the nanoparticle uptake still remains a debatable subject. Positive surface charge can provoke strong electrostatic attraction of nanoparticles in the negatively charged regions of plasma membrane and adsorption and internalization of nanoparticles [33; 34]. At the same time ca. 100 nm (by hydrodynamic size) negatively charged nanoparticles were efficiently absorbed by Caco-2 and epithelial MDCK cells [35–38]. Generally, nanoparticles with stronger zeta potential regardless of its sign exhibited better uptake by phagocytic cells. At the same time positively charged nanoparticles are always absorbed more efficiently than negatively charged ones [33]. Our results also demonstrate that positively charged encapsulated QDs are better absorbed by cells and the shift of zeta potential to neutral values decreases absorption efficiency.

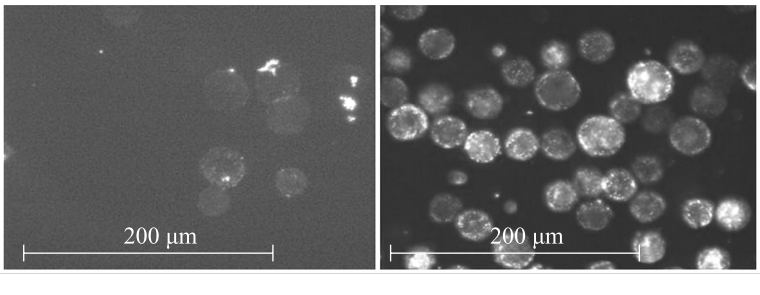

Fig. 2. Representative fluorescence images of EAC cells stained with (−)QDs (left) and (+)QDs (right)

In order to determine how the surface charge of QDs affects cell labeling, we examined cellular staining using (+/−)QDs with pH-tunable zeta potential. Figure 3 shows that while (−)QDs and (+)QDs have strongly negative and positive zeta potentials respectively in the wide range of pH, ξ value of (+/−)QDs varies from ca. −20 mV at pH >10 to +30 mV at pH < 5. The zwitterions on the surface of (+/−)QDs formed by paired quaternary amine and carboxyl groups provide different surface charge to the whole QD depending on the degree of carboxyl group deprotonation at different pH.

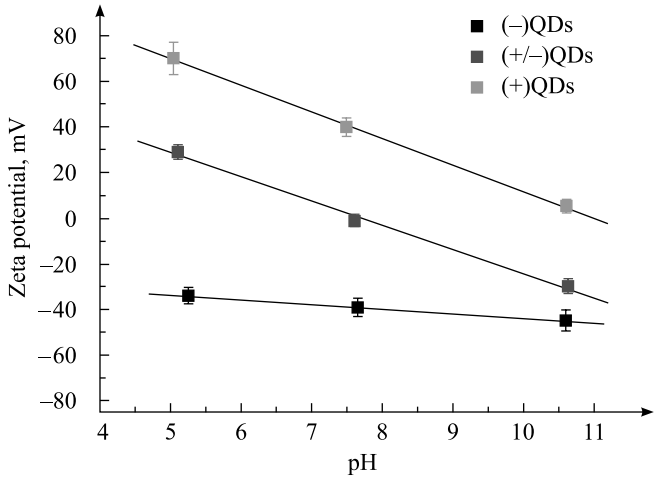

Fig. 3. The influence of pH on zeta potential of (−)QDs, (+)QDs and (+/−)QDs in different buffers. Dashed lines are linear fitting for corresponding experimental points

Figure 4 demonstrates that pH value has significant influence on the cell labeling with (+/−)QDs.

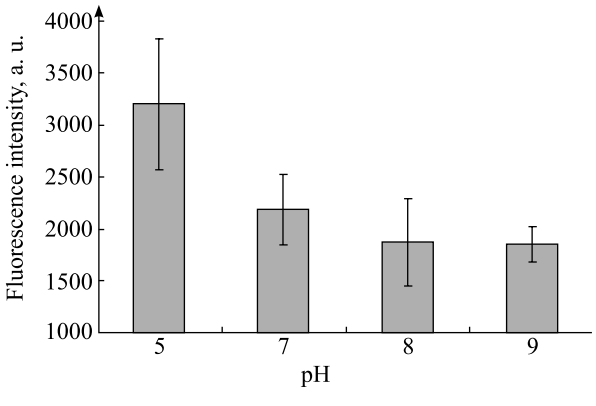

Fig. 4. pH-Dependent EAC cell staining with (+/−)QDs measured by fluorescence intensity ($n = 4$)

From fig. 4 we see that pH level has remarkable influence on the cellular staining with (+/−)QDs. These QDs interact with cells more efficiently in acidic solutions than in neutral or basic media. Although 98–100 % of EAC cells were stained with (+/−)QDs at all studied pH levels, the total amount of bound QDs (fluorescence intensity) was strongly pH-dependent. Tumor microenvironment is known to be acidic due to the abnormal metabolism of glucose and lactic acid production [38; 39] and the enhanced activity of proton transporters that pump out protons from the cells into the extracellular space [40–42]. Thus, positive zeta potential of (+/−)QDs in tumor tissues can increase and the nanoparticles will be better absorbed by tumor cells in comparison to normal tissues.

Besides the influence of zeta potential on staining efficiency, its possible effect on the cytotoxicity of encapsulated QDs was also considered. Figure 5 demonstrates that (−)QDs, (+)QDs and (+/−)QDs do not show cytotoxicity during 4 h, but promote cell death after 24 and 48 h incubation.

To date different mechanisms were proposed to explain possible cytotoxicity of CdSe/ZnS QDs, including the release of Zn^{2+}, Cd^{2+} or Se^{2-} ions that have negative effect on cells [43–45]. The mechanism of cytotoxicity can involve active oxygen forms, changes in permittivity of mitochondrial membranes, triggering of DNA damage and induction of apoptosis and necrosis [46–50]. QDs were also shown to be able to generate active oxygen forms upon photoexcitation in *Escherichia coli* stained with QDs [45]. Our results did not provide

clear evidence that cytotoxicity of QDs depends on their zeta potential. While after 24 h of incubation there was the correlation between decreased cytotoxicity of QDs and stronger positive zeta potential, the results of 48 h incubation did not exhibit such correlation. Taking into account that positive zeta potential of QDs enhances their absorption by cells, we assume that QDs' cytotoxicity does not depend on the fact, whether QDs are absorbed by cells, bound to the cell membrane or located outside the cells in the growth media.

Analysis of the fluorescence images shows that significant portion of QDs is localized near the cell membrane. In order to establish, whether QDs were internalized or attached to the outer side of the cell membrane, we treated cells after the QDs' uptake with Trypan blue. Figure 6 shows the effect of Trypan blue on the fluorescence of EAC cells stained with (−)QDs and (+)QDs.

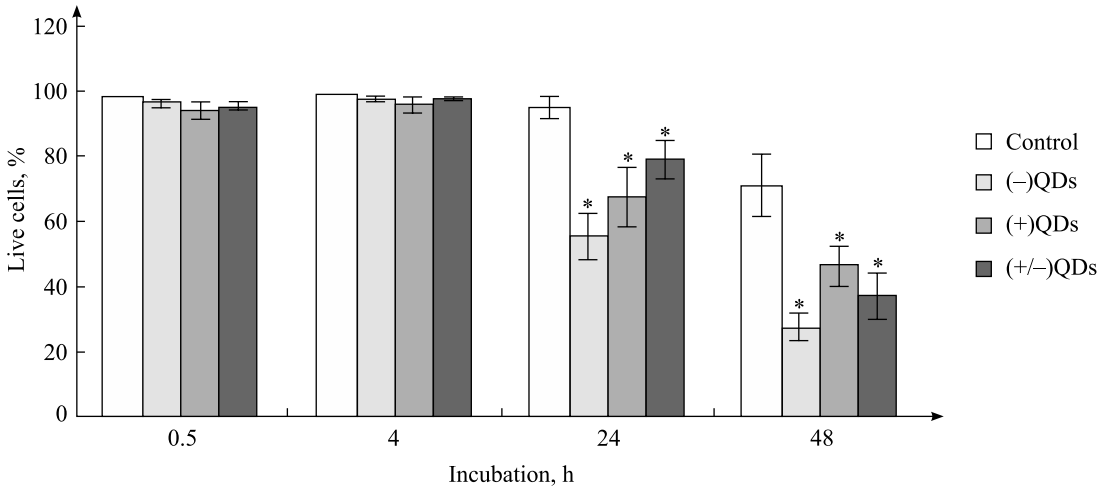

Fig. 5. Viability of EAC cells stained with (−)QDs, (+)QDs, (+/−)QDs during 48 h incubation

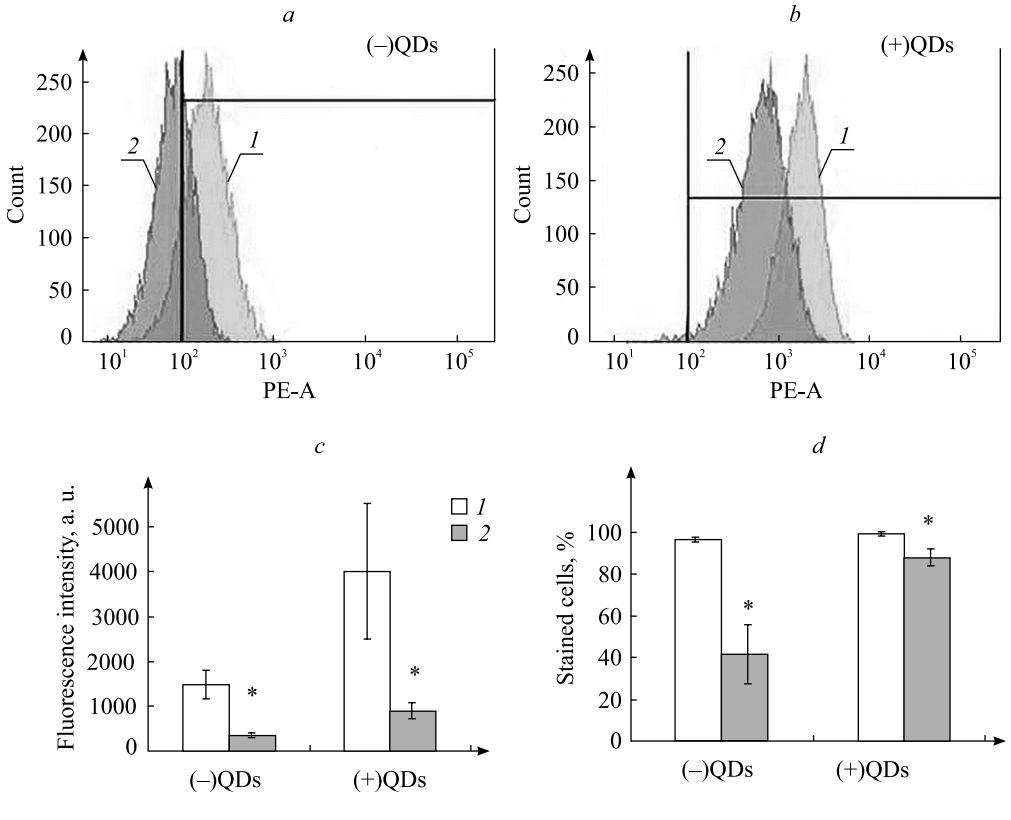

Fig. 6. Flow cytometry histograms (*a*, *b*), QDs fluorescence intensity (*c*) and percentage of stained cells (*d*) of EAC cells stained 30 min with (−)QDs and (+)QDs and treated with Trypan blue (*1* – before Trypan blue treatment, *2* – after Trypan blue treatment); **p* (1–2) < 0.05 according to the Mann – Whitney test (*n* = 4)

Trypan blue is known to quench the extracellular fluorescence of organic dyes [51; 52], surface-associated QDs and QDs in dead cells but has no effect on QDs internalized by live cells [53]. Figure 6 shows that cells stained with (+)QD have 2–3 times more intensive fluorescence signal in comparison to (−)QD. In both cases Trypan blue treatment results in ca. 4-fold quenching of QDs' fluorescence. Such quenching was not caused by the cell death, since data on fig. 6 demonstrates weak QDs' cytotoxicity. Therefore, the decrease of fluorescence signal can be explained by Trypan blue quenching of QDs localized on the outer side of the cell membrane. The difference between fluorescence signal before and after the treatment with Trypan blue corresponds to the amount of QDs attached to the outer side of the cell membrane. This difference is 2.8 times larger for cells stained with (+)QDs in comparison to (−)QDs which points to much larger amount of (+)QDs bound to the outer side of membrane.

After the quenching of extracellular fluorescence by Trypan blue cells stained with (+)QDs are still much brighter that in case of (−)QDs (see fig. 6). We may conclude that positively charged QDs are better adsorbed on the cell membrane and internalized by cells than negatively charged QDs. Positively charged QDs demonstrate high uptake by different human and animal cells. Studying cellular uptake of (+)QDs by human peripheral blood leucocytes subpopulations we observed that (+)QDs were able to label 90–100 % of all types of examined cells (neutrophils, monocytes, lymphocytes) in the serum-free medium. Additionally we were able to successfully label different tumor cells with (+)QDs including mouse Erlich ascites and hepatoma 22a, rat glioma C6 and human A549 (data not shown).

Figure 7 shows the level and fluorescence intensity of EAC cells stained with both CTV and QDs by 48 h incubation. CTV is not released from the cell by exocytosis and is homogeneously distributed between the daughter cells during division.

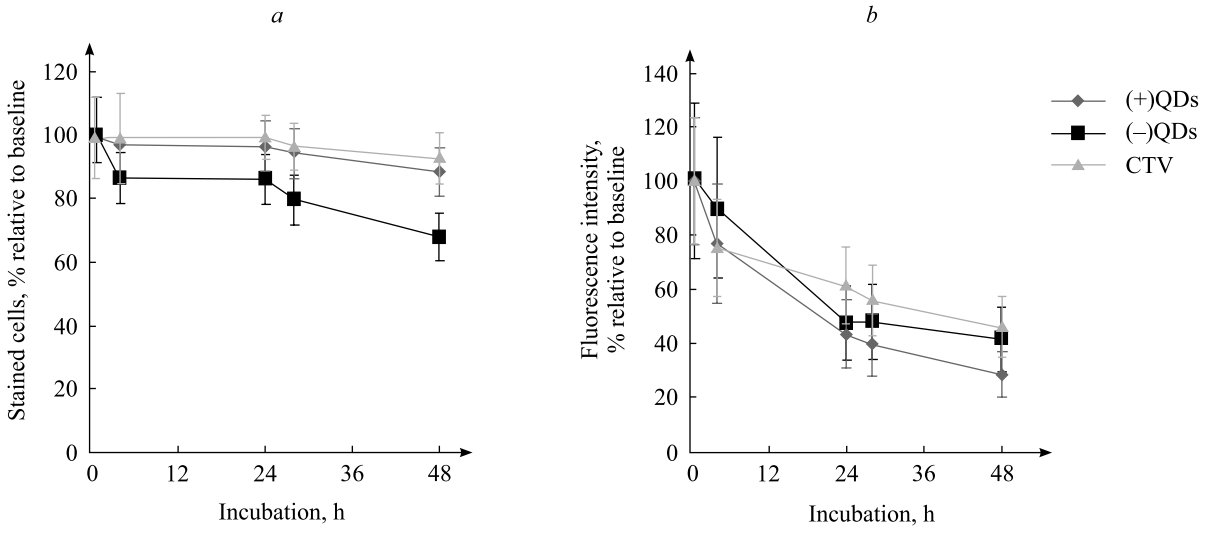

Fig. 7. Percentage of EAC cells stained with (+)QDs or (−)QDs during 48 h incubation *in vitro* ($n = 4$) (*a*). Fluorescence signal from EAC cells stained with (+)QDs or (−)QDs during 48 h incubation *in vitro* ($n = 4$) (*b*)

Cells were stained with QDs of different surface charge and CTV for 20 min, washed and cultivated in CTV- and QDs-free Dulbecco's modified Eagle's medium for 2 days in order to estimate the retention time of the fluorescence signal in living cells.

Fluorescence intensity of CTV decreases during 48 h of incubation period, what reflects the proliferation activity of EAC cells. Data analysis performed with ModFit software revealed that most cells divided 1–2 times and belonged to the second and third generations. Intensity dynamics of fluorescence signal in cells stained with (−)QDs and (+)QDs is similar to CTV, what points to the fact that cell division is a major factor that causes temporal decrease of the fluorescence intensity during 48 h incubation period. However, during the incubation period the amount of cells labeled by (−)QDs decreased for ca. 30 %, while the same parameter for (+)QDs and CTV changed insignificantly, what might be probably attributed to less efficient (−)QDs uptake by cells in comparison to positively charged QDs. Since fluorescence signal in the case of QDs decreases slightly faster with incubation time than in the case of CTV, the decrease of the signal cannot be solely attributed to the cell division. For example, different cellular models demonstrated the decrease of QDs' fluorescence due to exocytosis [37; 54; 55] and even to the chemical degradation of nanoparticles [56]. Further studies are required to determine exact mechanisms of fluorescence degradation in different cell cultures, which are important for practical applications of highly luminescent QDs as non-specific cell markers or staining agents.

Conclusions

Encapsulation of highly luminescent CdSe/ZnS quantum dots with chemically modified poly(maleic anhydride-alt-1-tetradecene) by (2-aminoethyl)trimethylammonium chloride allowed obtaining non-specific luminescent stains with controlled zeta potential through the formation of surface zwitterions. The efficiency of the cellular uptake of zwitterionic quantum dots was shown to be dependent on their zeta potential. In comparison to negatively charged quantum dots positively charged ones are better absorbed and intrernalized by cells. Negatively charged quantum dots tend to bind mainly to a cellular membrane. We did not observe any noticeable zeta potential-dependent toxicity of zwitterionic QDs within few hours. Long-term incubation of cells stained with zwitterionic quantum dots results in the decrease of the fluorescence signal mainly due to the cell proliferation. Highly luminescent quantum dots encapsulated with zwitterionic amphiphilic polymer can be considered as promising non-specific cell-staining agents with charge-controlled nanoparticle-cell interaction.

References

1. Liu J., Lau S. K., Varma V. A., et al. Multiplexed detection and characterization of rare tumor cells in Hodgkin's lymphoma with multicolor quantum dots. *Anal. Chem*. 2010. Vol. 82, issue 14. P. 6237–6243. DOI: 10.1021/ac101065b.

2. Yang X.-Q., Chen C., Peng C.-W., et al. Quantum dot-based quantitative immunofluorescence detection and spectrum analysis of epidermal growth factor receptor in breast cancer tissue arrays. *Int. J. Nanomedicine*. 2011. Vol. 6. P. 2265–2273. DOI: 10.2147/IJN.S24161.

3. Lee J., Kwon Y.-J., Choi Y., et al. Quantum Dot-Based Screening System for Discovery of G Protein-Coupled Receptor Agonists. *ChemBioChem*. 2012. Vol. 13, issue 10. P. 1503–1508. DOI: 10.1002/cbic.201200128.

4. Kairdolf B. A., Smith A. M., Stokes T. H., et al. Semiconductor Quantum Dots for Bioimaging and Biodiagnostic Applications. *Annu. Rev. Anal. Chem*. 2013. Vol. 6. P. 143–162. DOI: 10.1146/annurev-anchem-060908-155136.

5. Pellegrino T., Manna L., Kudera S., et al. Hydrophobic Nanocrystals Coated with an Amphiphilic Polymer Shell: a General Route to Water Soluble Nanocrystals. *Nano Lett.* 2004. Vol. 4, issue 4. P. 703–707. DOI: 10.1021/nl035172j.

6. Yu W. W., Chang E., Falkner J. C., et al. Forming biocompatible and nonaggregated nanocrystals in water using amphiphilic polymers. *J. Am. Chem. Soc.* 2007. Vol. 129, issue 10. P. 2871–2879. DOI: 10.1021/ja067184n.

7. Liu W., Choi H. S., Zimmer J. P., et al. Compact cysteine-coated CdSe(ZnCdS) quantum dots for in vivo applications. *J. Am. Chem. Soc*. 2007. Vol. 129, issue 47. P. 14530–14531. DOI: 10.1021/ja073790m.

8. Lin C.-A. J., Sperling R. A., Li J. K., et al. Design of an amphiphilic polymer for nanoparticle coating and functionalization. *Small*. 2008. Vol. 4, issue 3. P. 334–341. DOI: 10.1002/smll.200700654.

9. Smith A. M., Nie S. Minimizing the hydrodynamic size of quantum dots with multifunctional multidentate polymer ligands. *J. Am. Chem. Soc*. 2008. Vol. 130, issue 34. P. 11278–11279. DOI: 10.1021/ja804306c.

10. Lees E. E., Nguyen T.-L., Clayton A. H. A., et al. The preparation of colloidally stable, water-soluble, biocompatible, semiconductor nanocrystals with a small hydrodynamic diameter. *ACS Nano*. 2009. Vol. 3, issue 5. P. 1121–1128. DOI: 10.1021/nn900144n.

11. Pochard I., Boisvert J.-P., Persello J., et al. Surface charge, effective charge and dispersion/aggregation properties of nanoparticles. *Polym. Int*. 2003. Vol. 52, issue 4. P. 619–624. DOI: 10.1002/pi.1008.

12. Villanueva A., Cañete M., Roca A. G., et al. The influence of surface functionalization on the enhanced internalization of magnetic nanoparticles in cancer cells. *Nanotechnology*. 2009. Vol. 20, No. 11. P. 115103. DOI: 10.1088/0957-4484/20/11/115103.

13. Wilhelm C., Billotey C., Roger J., et al. Intracellular uptake of anionic superparamagnetic nanoparticles as a function of their surface coating. *Biomaterials*. 2003. Vol. 24, issue 6. P. 1001–1011. DOI: 10.1016/S0142-9612(02)00440-4.

14. Martin A. L., Bernas L. M., Rutt B. K., et al. Enhanced Cell Uptake of Superparamagnetic Iron Oxide Nanoparticles Functionalized with Dendritic Guanidines. *Bioconjug. Chem*. 2008. Vol. 19, issue 12. P. 2375–2384. DOI: 10.1021/bc800209u.

15. Park K. D., Kim Y. S., Han D. K., et al. Bacterial adhesion on PEG modified polyurethane surfaces. *Biomaterials*. 1998. Vol. 19, issue 719. P. 851–859.

16. Mei B. C., Susumu K., Medintz I. L., et al. Polyethylene glycol-based bidentate ligands to enhance quantum dot and gold nanoparticle stability in biological media. *Nat. Protoc*. 2009. Vol. 4, issue 3. P. 412–423. DOI: 10.1038/nprot.2008.243.

17. Mattoussi H., Palui G., Na H. B. Luminescent quantum dots as platforms for probing *in vitro* and *in vivo* biological processes. *Adv. Drug Deliv. Rev*. 2012. Vol. 64, issue 2. P. 138–166. DOI: 10.1016/j.addr.2011.09.011.

18. Liu W., Howarth M., Greytak A. B., et al. Compact biocompatible quantum dots functionalized for cellular imaging. *J. Am. Chem. Soc*. 2008. Vol. 130, issue 4. P. 1274–1284. DOI: 10.1021/ja076069p.

19. Park J., Nam J., Won N., et al. Compact and Stable Quantum Dots with Positive, Negative, or Zwitterionic Surface: Specific Cell Interactions and Non-Specific Adsorptions by the Surface Charges. *Adv. Funct. Mater*. 2011. Vol. 21, issue 9. P. 1558–1566. DOI: 10.1002/adfm.201001924.

20. Aldeek F., Safi M., Zhan N., et al. Understanding the Self-Assembly of Proteins onto Gold Nanoparticles and Quantum Dots Driven by Metal-Histidine Coordination. *ACS Nano*. 2013. Vol. 7, issue 11. P. 10197–10210. DOI: 10.1021/nn404479h.

21. Agarwal R., Domowicz M. S., Schwartz N. B., et al. Delivery and Tracking of Quantum Dot Peptide Bioconjugates in an Intact Developing Avian Brain. *ACS Chem. Neurosci*. 2015. Vol. 6, issue 3. P. 494–504. DOI: 10.1021/acschemneuro.5b00022.

22. Yezhelyev M. V., Qi L., O'Regan R. M., et al. Proton-Sponge Coated Quantum Dots for siRNA Delivery and Intracellular Imaging. *J. Am. Chem. Soc.* 2008. Vol. 130, issue 28. P. 9006–9012. DOI: 10.1021/ja800086u.

23. Wang W., Ji X., Kapur A., et al. A Multifunctional Polymer Combining the Imidazole and Zwitterion Motifs as a Biocompatible Compact Coating for Quantum Dots. *J. Am. Chem. Soc*. 2015. Vol. 137, issue 44. P. 14158–14172. DOI: 10.1021/jacs.5b08915.

24. Chithrani B. D., Ghazani A. A., Chan W. C. W. Determining the Size and Shape Dependence of Gold Nanoparticle Uptake into Mammalian Cells. *Nano Lett.* 2006. Vol. 6, issue 4. P. 662–668. DOI: 10.1021/nl052396o.

25. Jiang X., Dausend J., Hafner M., et al. Specific Effects of Surface Amines on Polystyrene Nanoparticles in their Interactions with Mesenchymal Stem Cells. *Biomacromolecules*. 2010. Vol. 11, issue 3. P. 748–753. DOI: 10.1021/bm901348z.

26. Silver J., Ou W. Photoactivation of Quantum Dot Fluorescence Following Endocytosis. *Nano Lett*. 2005. Vol. 5, issue 7. P. 1445–1449.

27. Delehanty J. B., Medintz I. L., Pons T., et al. Self-Assembled Quantum Dot-Peptide Bioconjugates for Selective Intracellular Delivery. *Bioconjug. Chem*. 2006. Vol. 17, issue 4. P. 920–927. DOI: 10.1021/bc060044i.

28. Jiang W., Kim B .Y. S., Rutka J. T., et al. Nanoparticle-mediated cellular response is size-dependent. *Nat. Nanotechnol*. 2008. Vol. 3, issue 3. P. 145–150. DOI: 10.1038/nnano.2008.30.

29. Jiang X., Röcker C., Hafner M., et al. Endo- and Exocytosis of Zwitterionic Quantum Dot Nanoparticles by Live HeLa Cells. *ACS Nano*. 2010. Vol. 4, issue 11. P. 6787–6797. DOI: 10.1021/nn101277w.

30. Geelen T., Yeo S. Y., Paulis L. E. M., et al. Internalization of paramagnetic phosphatidylserine-containing liposomes by macrophages. *J. Nanobiotechnol*. 2012. Vol. 10. P. 37. DOI: 10.1186/1477-3155-10-37.

31. Murphy J. E., Tacon D., Tedbury P. R., et al. LOX-1 scavenger receptor mediates calcium-dependent recognition of phosphatidylserine and apoptotic cells. *Biochem. J*. 2006. Vol. 393, issue 1. P. 107–115. DOI: 10.1042/BJ20051166.

32. Yamashita T. Ca^{2+}-dependent regulation of synaptic vesicle endocytosis. *Neurosci. Res.* 2012. Vol. 73, issue 1. P. 1–7. DOI: 10.1016/j.neures.2012.02.012.

33. He C., Hu Y., Yin L., et al. Effects of particle size and surface charge on cellular uptake and biodistribution of polymeric nanoparticles. *Biomaterials*. 2010. Vol. 31, issue 13. P. 3657–3666. DOI: 10.1016/j.biomaterials.2010.01.065.

34. Gu Y., Sun W., Wang G., et al. Single Particle Orientation and Rotation Tracking Discloses Distinctive Rotational Dynamics of Drug Delivery Vectors on Live Cell Membranes. *J. Am. Chem. Soc*. 2011. Vol. 133, issue 15. P. 5720–5723. DOI: 10.1021/ja200603x.

35. Song Q., Wang X., Hu Q., et al. Cellular internalization pathway and transcellular transport of pegylated polyester nanoparticles in Caco-2 cells. *Int. J. Pharm*. 2013. Vol. 445, issues 1/2. P. 58–68. DOI: 10.1016/j.ijpharm.2013.01.060.

36. He B., Lin P., Jia Z., et al. The transport mechanisms of polymer nanoparticles in Caco-2 epithelial cells. *Biomaterials*. 2013. Vol. 34, issue 25. P. 6082–6098. DOI: 10.1016/j.biomaterials.2013.04.053.

37. He B., Jia Z., Du W., et al. The transport pathways of polymer nanoparticles in MDCK epithelial cells. *Biomaterials*. 2013. Vol. 34, issue 17. P. 4309–4326. DOI: 10.1016/j.biomaterials.2013.01.100.

38. Schornack P. A., Gillies R. J. Contributions of Cell Metabolism and H^+ Diffusion to the Acidic pH of Tumors. *Neoplasia*. 2003. Vol. 5, issue 2. P. 135–145.

39. Harguindey S., Orive G., Luis Pedraz J., et al. The role of pH dynamics and the Na^+/H^+ antiporter in the etiopathogenesis and treatment of cancer. Two faces of the same coin-one single nature. *Biochim. Biophys. Acta. Rev. Cancer*. 2005. Vol. 1756, issue 1. P. 1–24. DOI: 10.1016/j.bbcan.2005.06.004.

40. Barar J., Omidi Y. Dysregulated pH in tumor microenvironment checkmates cancer therapy. *BioImpacts*. 2013. Vol. 3, issue 4. P. 149–162. DOI: 10.5681/bi.2013.036.

41. Reshkin S. J., Greco M. R., Cardone R. A. Role of pH_i, and proton transporters in oncogene-driven neoplastic transformation. *Phil. Trans. R. Soc. B*. 2014. Vol. 369, issue 1638. Article ID: 20130100. DOI: 10.1098/rstb.2013.0100.

42. Amith S. R., Wilkinson J. M., Fliegel L. Assessing Na^+/H^+ exchange and cell effector functionality in metastatic breast cancer. *Biochim. Open*. 2016. Vol. 2. P. 16–23. DOI: 10.1016/j.biopen.2016.01.001.

43. Corazzari I., Gilardino A., Dalmazzo S., et al. Localization of CdSe/ZnS quantum dots in the lysosomal acidic compartment of cultured neurons and its impact on viability: Potential role of ion release. *Toxicol. Vitr*. 2013. Vol. 27, issue 2. P. 752–759. DOI: 10.1016/j.tiv.2012.12.016.

44. Mahendra S., Zhu H., Colvin V. L., et al. Quantum Dot Weathering Results in Microbial Toxicity. *Environ. Sci. Technol*. 2008. Vol. 42, issue 24. P. 9424–9430.

45. Kauffer F.-A., Merlin C., Balan L., et al. Incidence of the core composition on the stability, the ROS production and the toxicity of CdSe quantum dots. *J. Hazard. Mater*. 2014. Vol. 268. P. 246–255. DOI: 10.1016/j.jhazmat.2014.01.029.

46. Singh B. R., Singh B. N., Khan W., et al. ROS-mediated apoptotic cell death in prostate cancer LNCaP cells induced by biosurfactant stabilized CdS quantum dots. *Biomaterials*. 2012. Vol. 33, issue 23. P. 5753–5767. DOI: 10.1016/j.biomaterials.2012.04.045.

47. Chen L., Miao Y., Chen L., et al. The role of elevated autophagy on the synaptic plasticity impairment caused by CdSe/ZnS quantum dots. *Biomaterials*. 2013. Vol. 34, issue 38. P. 10172–10181. DOI: 10.1016/j.biomaterials.2013.09.048.

48. Nguyen K. C., Willmore W. G., Tayabali A. F. Cadmium telluride quantum dots cause oxidative stress leading to extrinsic and intrinsic apoptosis in hepatocellular carcinoma HepG2 cells. *Toxicology*. 2013. Vol. 306. P. 114–123. DOI: 10.1016/j.tox.2013.02.010.

49. Zhang T., Wang Y., Kong L., et al. Threshold Dose of Three Types of Quantum Dots (QDs) Induces Oxidative Stress Triggers DNA Damage and Apoptosis in Mouse Fibroblast L929 Cells. *Int. J. Environ. Res. Public Health.* 2015. Vol. 12, issue 10. P. 13435–13454. DOI: 10.3390/ijerph121013435.

50. Lai L., Jin J.-C., Xu Z.-Q., et al. Necrotic cell death induced by the protein-mediated intercellular uptake of CdTe quantum dots. *Chemosphere*. 2015. Vol. 135. P. 240–249. DOI: 10.1016/j.chemosphere.2015.04.044.

51. Busetto S., Trevisan E., Patriarca P., et al. A single-step, sensitive flow cytofluorometric assay for the simultaneous assessment of membrane-bound and ingested Candida albicans in phagocytosing neutrophils. *Cytometry*. 2004. Vol. 58A, issue 2. P. 201–206. DOI: 10.1002/cyto.a.20014.

52. Avelar-Freitas B. A., Almeida V. G., Pinto M. C. X., et al. Trypan blue exclusion assay by flow cytometry. *Braz. J. Med. Biol. Res*. 2014. Vol. 47, issue 4. P. 307–315. DOI: 10.1590/1414-431X20143437.

53. Terpinskaya T. I., Zhavnerko G. K., Yashin K. D., et al. Interaction of fluorescent semiconductor nanoparticles with tumor cells. *Nanotechnol. Russ*. 2015. Vol. 10, issues 3/4. P. 303–310. DOI: 10.1134/S1995078015020196.

54. Ranjbarvaziri S., Kiani S., Akhlaghi A., et al. Quantum dot labeling using positive charged peptides in human hematopoetic and mesenchymal stem cells. *Biomaterials*. 2011. Vol. 32, issue 22. P. 5195–5205. DOI: 10.1016/j.biomaterials.2011.04.004.

55. Bae Y. M., Park Y. I., Nam S. H., et al. Endocytosis, intracellular transport, and exocytosis of lanthanide-doped upconverting nanoparticles in single living cells. *Biomaterials*. 2012. Vol. 33, issue 35. P. 9080–9086. DOI: 10.1016/j.biomaterials.2012.08.039.

56. Pi Q. M., Zhang W. J., Zhou G. D., et al. Degradation or excretion of quantum dots in mouse embryonic stem cells. *BMC Biotechnol*. 2010. Vol. 10. P. 36. DOI: 10.1186/1472-6750-10-36.

Received by editorial board 22.11.2017.